

Inverse modified differential equations for discovery of dynamics

Aiqing Zhu^{1,2}, Pengzhan Jin^{1,2}, Beibei Zhu³, and Yifa Tang^{1,2,*}

¹LSEC, ICMSEC, Academy of Mathematics and Systems Science, Chinese Academy of Sciences, Beijing 100190, China

²School of Mathematical Sciences, University of Chinese Academy of Sciences, Beijing 100049, China

³School of Mathematics and Physics, University of Science and Technology Beijing, Beijing 100083, China

*Email address: tyf@lsec.cc.ac.cn

Abstract

The combination of numerical integration and deep learning, i.e., ODE-net, has been successfully employed in a variety of applications. In this work, we introduce inverse modified differential equations (IMDE) to contribute to the behaviour and error analysis of discovery of dynamics using ODE-net. It is shown that the difference between the learned ODE and the truncated IMDE is bounded by the sum of learning loss and a discrepancy which can be made sub exponentially small in the data step size. In addition, we deduce that the total error of ODE-net is bounded by the sum of discrete error and learning loss. Furthermore, with the help of IMDE, theoretical results on learning Hamiltonian system are derived. Several experiments are performed to numerically verify our theoretical results.

Key words. Deep learning, Data-driven discovery, ODE-net, Modified equations, Error estimation, Hamiltonian system.

1 Introduction

Identification of nonlinear system is a significant task existing in diverse applications, for example, [7, 45]. Neural network has become a powerful approach for such task, and a series of continuous models combined numerical integrator and neural networks had already been developed and implemented to learn hidden dynamics decades ago [1, 22, 41, 42]. Recently, neural networks is experiencing a renaissance with the growth of available data and computing resources. At the same time, many researchers paid attention to the connection between dynamical systems and deep neural networks and have done many related work in terms of algorithms, architectures and applications [10, 13, 14, 35]. In particular, the continuous models has again attracted more and more attention and several ODE based models have been developed for discovery of hidden dynamics [6, 10, 34, 38, 51].

Although these learning models have been successfully employed, rigorous analysis of these approaches is still under investigation. In [12, 32], rigorous framework was established to derive estimation of grid error for linear multistep neural network (LMNet) [38]. It is proved that the grid error is bounded by the sum of discrete error and approximation error under auxiliary initial conditions. In this work, we concentrate on the behaviour and analysis of general ODE-net for discovery of dynamics. Here, the unknown governing vector fields are approximated by neural networks with given several phase points as training set. The training process is to minimize the difference between real states and predicted outputs of an ODE solver.

The main ingredient of this work is formal analysis [18]. Historically, modified differential equation is an important tool for understanding the numerical behavior of ordinary differential equation [15, 19, 43, 50]. The methodology is to interpret the numerical solution as the exact solution of a perturbed equation. In addition, modified integrator [9] was developed for high order integration. They tried to search a perturbed differential equation in which numerical solution matches the exact solution. In this paper, we use the same idea as modified integrator but for analysis of discovery using ODE-net. It is demonstrated that training ODE-net returns an

approximation of the perturbed equation. We name the obtained perturbed equation as inverse modified differential equation (IMDE) since discovery is an inverse problem.

We first consider the IMDE for general ODE solver and prove that several compositions of a numerical integrator has the same IMDE as the numerical integrator itself. In addition, this approach can be directly applied to linear multistep method, results in explicit recursion formula for LMNet. Furthermore, learning Hamiltonian system is discussed. It is found that for a Hamiltonian system, the IMDE based on the symplectic integrator is still a Hamiltonian system.

The formal series expressing IMDE does not converge in general and has to be truncated. Following conventional truncation theory [5, 24, 25, 40], the truncation inequalities are tailored to IMDE scenario. It is shown that the difference can be made sub exponentially small provided the target vector field f is real analytic and bounded. With this result, we obtain the rigorous error analysis for discovery using ODE-net. In summary, We list below several statements derived via IMDE that will be documented in detail later:

- ODE-nets have almost certain approximation target, i.e., the difference between the learned vector field f_{net} and the truncation of the vector field of IMDE f_h^N is bounded by the sum of learning loss and a discrepancy which is sub exponentially small in the data step size.
- The error between the trained network f_{net} and the unknown vector field f is bounded by the sum of discrete error Ch^p and learning loss, where h is the discrete step size and p is the order of integrator.
- Both ODE-net using non-symplectic integrators and LMNet tend not to learn conservation laws theoretically.
- HNN with symplectic integrator have almost certain approximation target. While this conclusion is not always true for HNN with non-symplectic integrators.

The rest of this paper is organized as follows. In Section 2, we briefly present some necessary notations, numerical integration, modified differential equations and modified integrator, the existing ODE based network architectures including ODE-net, LMNet and HNN are also introduced. In Section 3, we investigate IMDEs for such learning models. In particular, learning Hamiltonian system is discussed. The error estimation for ODE-net are detailed in Section 4. In Section 5 several numerical results are provided to verify the theoretical findings. Section 6 contains a brief summary and several comments on the future work.

2 Preliminaries

Without loss of generality, the attention in this paper will be addressed to autonomous systems of first-order ordinary differential equations

$$\frac{d}{dt}y(t) = f(y(t)), \quad y(0) = x, \quad (1)$$

where $y(t) \in \mathbb{R}^N$ and $f : \mathbb{R}^N \rightarrow \mathbb{R}^N$ is Lipschitz continuous. The initial value is denoted as x in this paper. A non-autonomous system $\frac{d}{dt}y(t) = f(t, y(t), p)$ with parameters p can be brought into this form by appending the equation $\frac{d}{dt}t = 1$ and $\frac{d}{dp}t = 0$. Let $\phi_t(x)$ be the exact solution and $\Phi_h(x)$ be the numerical solution with discrete step h and initial condition $y(0) = x$, we will add the subscript f , denote ϕ_t as $\phi_{t,f}$ and Φ_h as $\Phi_{h,f}$ to emphasize specific differential equation. The choice for ODE solver in this paper is S compositions of a numerical integrator, i.e.,

$$\text{ODESolve}(x, f, T) = \underbrace{\Phi_{h,f} \circ \cdots \circ \Phi_{h,f}}_{S \text{ compositions}}(x) = (\Phi_{h,f})^S(x),$$

where $T = Sh$ with discrete step size h and composition number S .

2.1 Numerical integration: brief review

In the last few decades, several kinds of numerical integrations have been developed for ordinary differential equations, including Runge-Kutta methods and linear multistep methods. We recall some basic definitions and essential supporting results here. Refer to [8, 27, 28] for more presentations of integrators. Below we first present the concept of order and consistency.

Order. An integrator $\Phi_h(x)$ with discrete step h has order p , if for any sufficiently smooth equation (1) with arbitrary initial value x ,

$$\Phi_{h,f}(x) = \phi_{h,f}(x) + O(h^{p+1}).$$

Consistency. An integrator is consistent if it has order $p \geq 1$.

2.1.1 Runge-Kutta methods

Let b_i, a_{ij} ($i, j = 1, \dots, s$) be real numbers and let $c_i = \sum_{j=1}^s a_{ij}$. An s -stage Runge-Kutta method for (1) is defined as

$$\begin{aligned} k_i &= f \left(y_0 + h \sum_{j=1}^s a_{ij} k_j \right), \quad i = 1, \dots, s, \\ y_1 &= y_0 + h \sum_{i=1}^s b_i k_i, \end{aligned} \tag{2}$$

where the function f is given and $\Phi_{h,f}(y_0) = y_1$. The method is called explicit if $a_{ij} = 0$ for $i \leq j$ and implicit otherwise. For sufficiently small h , the nonlinear equation (2) for the slopes k_1, \dots, k_s has a local solution close to $f(y_0)$ guaranteed by Implicit Function Theorem.

Theorem 1. *The derivatives of the solution of a Runge-Kutta method (2), for $h = 0$, are given by*

$$y_1^{(q)}|_{h=0} = \sum_{|\tau|=q} \gamma(\tau) \cdot \alpha(\tau) \cdot \phi(\tau) \cdot F(\tau)(y_0).$$

Here, τ is called trees and $|\tau|$ is the order of τ (the number of vertices). $\gamma(\tau)$, $\phi(\tau)$, $\alpha(\tau)$ are positive integer coefficients, $F(\tau)(y)$ is called elementary differentials and typically composed of $f(y)$ and its derivatives.

$ \tau $	τ	$\gamma(\tau)$	$\alpha(\tau)$	$\phi(\tau)$	$F(\tau)$
1	\bullet	1	1	$\sum_i b_i$	f
2	$[\bullet]$	2	1	$\sum_{ij} b_i a_{ij}$	$f'f$
3	$[\bullet, \bullet]$	3	1	$\sum_{ijk} b_i a_{ij} a_{ik}$	$f''(f, f)$
3	$[[\bullet]]$	6	1	$\sum_{ijk} b_i a_{ij} a_{jk}$	$f'f'f$
4	$[\bullet, \bullet, \bullet]$	4	1	$\sum_{ijkl} b_i a_{ij} a_{ik} a_{il}$	$f'''(f, f, f)$
4	$[[\bullet], \bullet]$	8	3	$\sum_{ijkl} b_i a_{ij} a_{ik} a_{jl}$	$f''(f'f, f)$
4	$[[\bullet, \bullet]]$	12	1	$\sum_{ijkl} b_i a_{ij} a_{jk} a_{jl}$	$f'f''(f, f)$
4	$[[[\bullet]]]$	24	1	$\sum_{ijkl} b_i a_{ij} a_{jk} a_{kl}$	$f'f'f'f$

Table 1: Trees, elementary differentials and coefficients

Some $\gamma(\tau), \alpha(\tau), \phi(\tau), F(\tau)$ are reported in Table 1, more detailed proof and computation are shown in [27, Chapter III]. Due to Theorem 1, the formal expansion of a Runge-Kutta method with initial condition $y_0 = x$ is given by

$$\Phi_{h,f}(x) = y + h d_{1,f}(x) + h^2 d_{2,f}(x) + \dots,$$

where

$$d_{k,f}(x) = \frac{1}{k!} y_1^{(k)}|_{h=0} = \frac{1}{k!} \sum_{|\tau|=k} \gamma(\tau) \cdot \alpha(\tau) \cdot \phi(\tau) \cdot F(\tau)(x).$$

2.1.2 Linear multistep methods

For first order differential equations (1), linear multistep methods are defined by the formula

$$\sum_{m=0}^M \alpha_m y_m - h \sum_{m=0}^M \beta_m f(y_m) = 0, \tag{3}$$

where α_m, β_m are real parameters, $a_M \neq 0$ and $|\alpha_0| + |\beta_0| > 0$. The method (3) is explicit if $\beta_M = 0$, otherwise it is implicit. In [20], it is shown that weakly stable multistep methods are essentially equivalent to one-step methods.

Theorem 2. *Consider a weakly stable multistep method (3), there exists a unique formal expansion*

$$\Phi_{h,f}(x) = y + h d_{1,f}(x) + h^2 d_{2,f}(x) + \dots$$

such that

$$\sum_{m=0}^M \alpha_m \Phi_{mh,f}(x) = h \sum_{m=0}^M \beta_m f(\Phi_{mh,f}(x))$$

for arbitrary initial value x .

Here, $\Phi_{h,f}(x)$ is called “step-transition operator” [20], which also provides the formal expansion of linear multistep methods.

2.1.3 Symplectic integration methods

For even dimension N , denote the $N/2$ -by- $N/2$ identity matrix by I , and let

$$J = \begin{pmatrix} 0 & I \\ -I & 0 \end{pmatrix}.$$

Definition 1. *A differentiable map $g : U \rightarrow \mathbb{R}^N$ (where N is even and $U \subseteq \mathbb{R}^N$ is an open set) is called symplectic if*

$$g'(x)^T J g'(x) = J,$$

where $g'(x)$ is the Jacobian of $g(x)$.

A Hamiltonian system is given by

$$\frac{d}{dt}y = J^{-1} \nabla H(y), \quad y(0) = x, \quad (4)$$

where $y \in \mathbb{R}^N$ and H is the Hamiltonian typically representing the energy of (4) [2, 3]. Another remarkable property of Hamiltonian system is symplectic. In 1899, Poincaré proved that the exact solution of a Hamiltonian system (4) is a symplectic map [2, Section 38], i.e.,

$$\phi'_t(x)^T J \phi'_t(x) = J.$$

where $\phi'_t(x) = \frac{\partial \phi_t(x)}{\partial x}$ is the Jacobian of ϕ_t . Since the intrinsic symplecticity, it is natural to search for numerical methods that preserve this structure, i.e., make Φ_h be a symplectic map. There are some well-developed works on symplectic integration, see for example [16, 17, 27, 43]. It should be noticed that both linear multistep method and explicit Runge-Kutta method can not be always symplectic [27, 46].

2.1.4 Lie derivatives

Following [27], we briefly review Lie derivatives. Given equation (1), Lie derivative D is the differential operator defined by

$$Dg(y) = g'(y)f(y)$$

for $g : \mathbb{R}^N \rightarrow \mathbb{R}^M$. According to the chain rule, we have

$$\frac{d}{dt}g(\phi_{t,f}(x)) = (Dg)(\phi_{t,f}(x))$$

for arbitrary initial value x and thus obtain the Taylor series of $g(\phi_{t,f}(x))$ developed at $t = 0$:

$$g(\phi_{t,f}(x)) = \sum_{k=0}^{\infty} \frac{t^k}{k!} (D^k g)(x). \quad (5)$$

In particular, by setting $t = h$ and $g(y) = I_N(y) = y$, the identity map, it turns to the Taylor series of the exact solution $\phi_{h,f}$ itself, i.e.,

$$\begin{aligned}\phi_{h,f}(x) &= \sum_{k=0}^{\infty} \frac{h^k}{k!} (D^k I_N)(x) \\ &= x + hf(x) + \frac{h^2}{2} f'f(x) + \frac{h^3}{6} (f''(f, f)(x) + f'f'f(x)) \\ &\quad + \frac{h^4}{24} (f'''(f, f, f)(x) + 3f''(f'f, f)(x) + f'f''(f, f)(x) + f'f'f'f(x)) \\ &\quad + \dots\end{aligned}\tag{6}$$

Here, the notation $f'(x)$ for the derivative is a linear map (the Jacobian), the second derivative $f''(x)$ is a symmetric bilinear map and similarly for higher derivatives described as tensor.

2.2 Modified differential equations and modified integrator

Modified differential equation is a well-established tool for numerical treatment of ordinary differential equation. The approach is to search a perturbed differential equation

$$\frac{d}{dt} \tilde{y}(t) = f_h(\tilde{y}(t)) = f_0(\tilde{y}) + hf_1(\tilde{y}) + h^2 f_2(\tilde{y}) + \dots, \quad \tilde{y}(0) = x\tag{7}$$

such that $\Phi_{h,f}(x) = \phi_{t,f_h}(x)$ formally, where $\Phi_{h,f}(x)$ is the numerical solution of (1) and $\phi_{t,f_h}(x)$ is the exact solution of (7). Expanding $\phi_{t,f_h}(x)$ into a power series of h via substituting f_h and comparing equal powers of h with $\Phi_{h,f}(x)$ yields recursion formulas for f_k . Detailed computation procedure we refer to [27, Section 9].

Modified integrator is a approach for constructing high order methods via modified differential equations [9]. The idea is to find a perturbed differential equation

$$\frac{d}{dt} \tilde{y}(t) = f_h(\tilde{y}(t)) = f_0(\tilde{y}) + hf_1(\tilde{y}) + h^2 f_2(\tilde{y}) + \dots, \quad \tilde{y}(0) = x\tag{8}$$

such that $\Phi_{h,f_h}(x) = \phi_{t,f}(x)$ formally.

For implementation, we first expand the numerical solution $\Phi_{h,f_h}(x)$ as

$$\Phi_{h,f_h}(x) = x + hd_{1,f_h}(x) + h^2 d_{2,f_h}(x) + h^3 d_{3,f_h}(x) + \dots,\tag{9}$$

where the functions d_{j,f_h} are given and typically composed of f_h and its derivatives. For consistent integrators,

$$d_{1,f_h}(x) = f_h(x) = f_0(x) + hf_1(x) + h^2 f_2(x) + \dots.$$

In $h^i d_{i,f_h}(x)$, the powers of h of the terms containing f_k is at least $k + i$. Thus the coefficients of h^{k+1} in (9) is

$$f_k + \dots,$$

where the “ \dots ” indicates residual terms composed of f_j with $j \leq k - 1$ and their derivatives. By comparison of the coefficients of like powers of h in (6) and (9), unique functions f_k in (8) are obtained recursively. Here, the identity is understood in the sense of the formal power series in h . In particular, for a method of order p , the functions f_1, \dots, f_{p-1} vanish identically.

Theorem 3. *Suppose that the integrator $\Phi_h(x)$ with discrete step h is of order $p \geq 1$, more precisely,*

$$\Phi_{h,f}(x) = \phi_{h,f}(x) + h^{p+1} \delta_f(x) + O(h^{p+2}),$$

where $h^{p+1} \delta_f(x)$ is the leading term of the local truncation applied to equation (1). Then, the IMDE obeys

$$\frac{d}{dt} \tilde{y} = f_h(\tilde{y}) = f(\tilde{y}) + h^p f_p(\tilde{y}) + \dots,$$

where $f_p(y) = -\delta_f(y)$.

Proof. The function f_k is obtained from

$$\Phi_{h,f_h^k} = \phi_{h,f} - h^{k+1} f_k + O(h^{k+2}),$$

which concludes the proof. \square

Denote the truncation of series in (8) as

$$f_h^K(y) = \sum_{k=0}^K h^k f_k(y),$$

The above computation procedure implies that

$$\Phi_{h,f_h^K}(x) = \phi_{h,f}(x) + O(h^{K+2}),$$

which defines a numerical method of order $K + 1$ for (1).

2.3 ODE based neural networks

The discovery of dynamics is essentially a process of identifying the unknown vector field f (also known as dynamics) of a dynamical system (1) using provided information of the flow map on given phase points (typically are the states at equidistant time steps of a trajectory, and are written as $\{(x^i, \phi_{T,f}(x^i))\}_{i=1}^I$ in this paper for generality). Here, we assume that the state set is exact and the data step T is a sufficiently small constant.

Below we briefly recall existing data-driven discovery model using neural networks, including ODE-nets, Linear multistep neural networks and Hamiltonian neural networks.

2.3.1 ODE-nets

Recently, Neural ODE [10] is proposed as a continuous model by embedding a neural network into an ODE solver. Before the introduction of neural ODE, there were multiple pioneering efforts combining neural networks and ODE solver to discovery the hidden dynamics [1, 22, 41, 42]. In the literature, these models are known as ODE-nets. Using such models, the governing function f is approximated by neural networks via optimizing

$$\inf_{u \in \Gamma} \int_{\mathcal{X}} l(\text{ODESolve}(x, u, T), \phi_{T,f}(x)) dP(x). \quad (10)$$

Here $l(\cdot, \cdot)$ is a loss function that is minimized when its arguments are equal (a common choice for regression problem is the square loss $l(y, \hat{y}) = \|y - \hat{y}\|_2^2$). $P(x)$ is a probability measure on \mathcal{X} modelling the input distribution which is unknown in practice. In the setting of discovery, we sample training data $\{(x^i, \phi_{T,f}(x^i))\}_{i=1}^N$ and set $P(x)$ to be the empirical measure $P = \sum_{i=1}^I I^{-1} \delta_{x^i}$, yielding the empirical risk optimization problem

$$\inf_{u \in \Gamma} \frac{1}{I} \sum_{i=1}^I l(\text{ODESolve}(x^i, u, T), \phi_{T,f}(x^i)).$$

We denote the obtained neural network as f_{net} . The desired purpose is that f_{net} achieve small loss in the unknown data. Although most existing theoretical works fail to explain the performance, neural network framework have better generalization in practice.

2.3.2 Linear multistep neural networks

Linear multistep neural networks (LMNets), developed in [38], apply linear multistep methods and neural networks to discovery of dynamics by given state y on a trajectory at equidistant steps. For LMNets, the unknown f is replaced by neural networks in (3) and is learned by minimizing the residual

$$\inf_{u \in \Gamma} \sum_{i=0}^{I-M} \left\| \sum_{m=0}^M h^{-1} \alpha_m y_{i+m} - \sum_{m=0}^M \beta_m u(y_{i+m}) \right\|_2^2.$$

Here, $y_i = y(ih)$ with $i = 0, \dots, I$ is the given temporal data-snapshots. In [32], a frame work based on refined notions is established for convergence and stability analysis. Error estimation is enriched in [12], which indicates that the grid error is bounded by the sum discrete error and approximation error under auxiliary initial conditions.

2.3.3 Hamiltonian neural networks

Although ODE-nets have remarkable abilities to learn and generalize from data, there exists a vast amount of prior knowledge that is currently not being utilized. Encoding prior information into a learning algorithm have attracted increasing attention recently [30, 36, 39]. In this paper, we will investigate Hamiltonian neural networks (HNN) [6, 11, 23, 47], in which only the Hamiltonian H instead of the total vector field f is unknown and parameterized.

The methodology of HNN is to represent the Hamiltonian $H(y)$ by neural networks u and compute $J^{-1}\nabla u(y)$ via auto-differentiation. Subsequently, the approximation is obtained within ODE-net framework, i.e., minimizing the loss

$$\min_{u \in \Gamma} \frac{1}{I} \sum_{i=1}^I \left\| \text{ODESolve}(x^i, J^{-1}\nabla u, T) - \phi_{T, J^{-1}\nabla H}(x^i) \right\|_2^2,$$

where Γ is the set of neural networks. There have been many research works focusing on HNN with symplectic integration [11, 47, 48], this issue will be documented in detail later.

3 Inverse modified differential equations

Consider a very idealized assumption: the neural networks produce zero loss for complete data, i.e.,

$$\phi_{T,f}(x) = \text{ODESolve}(x, f_{\text{net}}, T).$$

Meanwhile, an ODE solver can be regarded as a one-step integrator with discrete step T , and there is a perturbed equation (8) formally obeys

$$\phi_{T,f}(x) = \text{ODESolve}(x, F_T, T).$$

Thus it is natural to expect that training an ODE-net returns an approximation of F_T . Similar discussion holds for LMNets and HNN. In this paper, we name the perturbed equation (8) as inverse modified differential equation (IMDE), since it is used for analysis of discovery. We will introduce the IMDE corresponding to the aforementioned learning models in this section and present rigorous analysis in next section.

3.1 Inverse modified differential equations for ODE-net

Detailed computation procedure of IMDE for one-step integrator has been presented in subsection 2.2. The ODE solver can be regarded as a one-step integrator with discrete step T . Thus it has the unique IMDE denoted as F_T^K such that

$$\text{ODESolve}(x, F_T^K, T) = \phi_{T,f}(x) + O(T^{K+2})$$

where $F_T^K(y) = \sum_{k=0}^K T^k F_k(y)$. Recall that the ODE solver is the fixed S compositions of the integrator Φ_{h, F_T^K} , i.e.,

$$\text{ODESolve}(x, F_T^K, T) = \left(\Phi_{h, F_T^K} \right)^S(x).$$

The following theorem indicates that the IMDE of Φ_h is coincide with the IMDE of the ODE solver.

Theorem 4. *For any fixed composition number S and truncation index K , there exist unique h -independent functions f_k for $0 \leq k \leq K$ such that, the numerical solution of*

$$\frac{d}{dt} \tilde{y} = f_h^K(\tilde{y}) = \sum_{k=0}^K h^k f_k(\tilde{y}),$$

satisfies

$$\Phi_{h, f_h^K}(x) = \phi_{h,f}(x) + O(h^{K+2})$$

and

$$\left(\Phi_{h, f_h^K} \right)^S(x) = \phi_{Sh,f}(x) + O(h^{K+2})$$

for arbitrary initial value x . Here the identity is understood in the sense of the formal power series in h .

Proof. The proof can be found in Appendix A. □

3.2 Inverse modified differential equations for LMNet

The formal expansion of $\Phi_{h,f_h}(x)$ for a linear multistep method also exists by Theorem 2, thus above computation can be directly applied to step-transition operators. Using Lie derivatives, we introduce a new approach to derive explicit recursion of IMDEs directly from the multistep formula (3).

Theorem 5. *Consider a weakly stable and consistent multistep method (3), there exist unique h -independent functions f_k for $0 \leq k \leq K$ such that $f_h^K = \sum_{k=0}^K h^k f_k$ satisfies*

$$\sum_{m=0}^M \alpha_m \phi_{mh,f}(x) = h \sum_{m=0}^M \beta_m f_h^K(\phi_{mh,f}(x)) + O(h^{K+2}) \quad (11)$$

for arbitrary initial value x . In particular, for $k \geq 0$, the functions f_k are given as

$$f_k(y) = \frac{1}{(\sum_{m=0}^M \beta_m)} \sum_{m=0}^M \alpha_m \frac{m^{k+1}}{(k+1)!} (D^k f)(y) - \frac{1}{(\sum_{m=0}^M \beta_m)} \sum_{m=0}^M \beta_m \sum_{j=1}^k \frac{m^j}{j!} (D^j f_{k-j})(y). \quad (12)$$

Here, the consistency requires

$$\sum_{m=0}^M \alpha_m = 0, \quad \sum_{m=0}^M m \cdot \alpha_m = \sum_{m=0}^M \beta_m,$$

and the weak stability requires

$$\sum_{m=0}^M m \cdot \alpha_m \neq 0,$$

which yields $\sum_{m=0}^M \beta_m \neq 0$ due to the consistency condition.

Proof. The proof can be found in Appendix B. □

3.3 Learning Hamiltonian system and HNN

For Hamiltonian system

$$\frac{d}{dt} y = J^{-1} \nabla H(y),$$

applying Theorem 4 yields a unique IMDE such that formally

$$\phi_{T,J^{-1}\nabla H}(x) = \text{ODESolve}(x, f_h, T).$$

Therefore, learning Hamiltonian system, or conservation law, requires the IMDE to be a Hamiltonian system, i.e., Jf_h is a potential field. This is not always true, we prove that IMDE based on the symplectic integrator is still a Hamiltonian system below.

Theorem 6. *Consider a Hamiltonian system with a smooth Hamiltonian H , if the integrator $\Phi_h(y)$ is symplectic, its IMDE is also a Hamiltonian system. More precisely, there locally exist smooth functions H_k , $k = 0, 1, 2, \dots$, such that*

$$f_k(y) = J^{-1} \nabla H_k(y).$$

Proof. This statement has been found in [9]. We provide a complete proof in Appendix C. □

Non-symplectic integrators can not guarantee that the IMDE is always Hamiltonian system. Thus ODE-net using non-symplectic integrators and LMNet tend not to learn conservation laws. We remark that both linear multistep method and explicit Runge-Kutta method can not be always symplectic [27, 46]. This statement was discussed in [23], while IMDE reveal this issue theoretically. To overcome this limitation, HNN [23] is proposed by imposing intrinsic Hamiltonian structure. Theorem 6 also indicates that HNN with symplectic integrator have certain approximation target. While this conclusion is not always true for HNN with non-symplectic integrators, using non-symplectic integrators could lead to excessive loss and uncertain results dominated by data distribution. Below We call the HNet with symplectic (non-symplectic) integrator as S-HNN (NS-HNN).

3.4 Discussion on uniqueness

We consider the differential equation

$$\begin{aligned}\frac{d}{dt}p &= a, \\ \frac{d}{dt}q &= \sin(p + b),\end{aligned}$$

with parameters a, b and initial value $(p(0), q(0)) = (p_0, q_0)$. The exact solution is given as

$$\begin{aligned}p(t) &= p_0 + at, \\ q(t) &= q_0 - \frac{1}{a}(\cos(p_0 + at + b) - \cos(p_0 + b)).\end{aligned}$$

When $t = \frac{2\pi}{a}$, we have

$$\begin{aligned}p &= p_0 + 2\pi, \\ q &= q_0.\end{aligned}$$

Thus, same exact solutions are obtained although the parameter b is different.

In addition, consider a linear equation

$$\frac{d}{dt}p = \lambda p$$

with parameter λ . Applying explicit Euler method twice yields

$$p_1 = (1 + \lambda h)^2 p_0 = (1 + (-2/h - \lambda)h)^2 p_0.$$

Same numerical solutions are obtained for parameter λ and $(-2/h - \lambda)$.

The above examples indicate non-uniqueness even smooth f . Formally, training ODE-nets returns an approximation of an IMDE. However, the constant hidden in the $O(h^{K+2})$ tend to infinity and the series (8) diverges in general. We need additional assumption for rigorous analysis. These issues will be discussed in next section.

4 Error analysis for discovery using ODE-net

To begin with, we introduce some notations. For a compact subset $\mathcal{K} \subset \mathbb{C}^N$, let $\mathcal{B}(x, r) \subset \mathbb{C}^N$ denote the complex ball of radius $r > 0$ centered at $x \in \mathbb{C}^N$ and define

$$\mathcal{B}(\mathcal{K}, r) = \bigcup_{x \in \mathcal{K}} \mathcal{B}(x, r).$$

We will work with l_∞ - norm on \mathbb{C}^N , denote $\|\cdot\| = \|\cdot\|_\infty$, and for a real analytic vector field f , define

$$\|f\|_{\mathcal{K}} = \sup_{x \in \mathcal{K}} \|f(x)\|.$$

Throughout this section, our conclusion is based on the following two assumptions:

The generalization assumption. For $x \in \mathbb{R}^N$, we assume that the learning models have good generalization near x in the complex space, more precisely, there exists r_1 such that

$$\|\text{ODESolve}(\cdot, f_{net}, Sh) - \phi_{Sh, f}(\cdot)\|_{\mathcal{B}(x, r_1)} \ll h^{p+1}$$

In this section, we will use this learning loss as the error bound.

The analyticity assumption. For $x \in \mathbb{R}^N$ and constant $r_2 > 0$, we assume that the target vector field f and the learned vector field f_{net} are real analytic and bounded by m on $\mathcal{B}(x, r_1 + r_2)$, i.e.,

$$\|f\|_{\mathcal{B}(x, r_1 + r_2)} \leq m, \quad \|f_{net}\|_{\mathcal{B}(x, r_1 + r_2)} \leq m. \quad (13)$$

Theorem 7. *Given an ODE solver which is S compositions of a Runge-Kutta method Φ_h with discrete step h . For $x \in \mathbb{R}^N$, suppose the assumptions are satisfied, then, for sufficiently small $h > 0$, there exist integer $K = K(h)$, and constants q, γ, c_1, c_2, C which depend on m, r_1, r_2 and the ODE solver, such that*

$$\begin{aligned}\|f_{net}(x) - f_h^K(x)\| &\leq c_1 e^{-\gamma/(Sh)^{1/q}} + C\mathcal{L}. \\ \|f_{net}(x) - f(x)\| &\leq c_2 h^p + C\mathcal{L},\end{aligned}$$

where $\mathcal{L} = \|\text{ODESolve}(\cdot, f_{net}, Sh) - \phi_{Sh, f}(\cdot)\|_{\mathcal{B}(x, r_1)} / Sh$.

Here, the generalization assumption is in some sense necessary. If the ODE solver is one composition of implicit Euler method, then, there is no information of f_{net} at x . Although quantifying the learning loss is still an open research problem, fortunately, neural network framework has better generalization in practice. The main disadvantage is the generalization assumption on complex ball, we conjecture that there is no essential difference between complex and real space. The analyticity assumption indicate boundness of derivatives of f due to Cauchy's estimate [44], more precisely,

$$\|f^{(k)}\|_{\mathcal{B}(x, r_1)} \leq k! m r_2^{-k}, \quad k \geq 0.$$

This assumption checks off the high-frequency solution and thus our results only hold for low-frequency discovery. In classical regression problems, training FNN first captures low-frequency components of the target function and then approximate the high-frequency [37, 49]. We conjecture that the implicit regularization are also applied to ODE-net and thus the analyticity assumption of f_{net} holds without any explicit regularization. Numerical results in Section 5 will validate both facts.

The requirement of Runge-kutta method is not necessary. For g, \hat{g} satisfy $\|g\|_{\mathcal{B}(\mathcal{K}, r)} \leq m, \|\hat{g}\|_{\mathcal{B}(\mathcal{K}, r)} \leq m$, we assume the numerical integrator $\Phi_h(y)$ satisfy

1. Analytic for $|h| \leq h_0 = b_1 r / m$ and $y \in \mathcal{K}$
 2. $\|\Phi_{h, \hat{g}} - \Phi_{h, g}\|_{\mathcal{K}} \leq b_2 h \|\hat{g} - g\|_{\mathcal{B}(\mathcal{K}, r)},$ for $|h| \leq h_0$.
 3. $\|\hat{g} - g\|_{\mathcal{K}} \leq \frac{1}{|h|} \|\Phi_{h, \hat{g}}(y) - \Phi_{h, g}(y)\|_{\mathcal{K}} + b_2 \frac{|h|}{h_0 - |h|} \|\hat{g} - g\|_{\mathcal{B}(\mathcal{K}, b_3 |h| m)},$ for $|h| \leq h_0$.
- (14)

Here, b_1, b_2, b_3 depend only on the method. Regarding an ODE solver as a one-step integrator, once it satisfies condition (14), then Theorem 7 holds.

5 Numerical results

In this section, we show numerical evidences consistent with the theoretical findings. The exact solutions are computed by very high order numerical integrators on very fine mesh. The order of error E with respect to discrete step h is calculated by $\log_2(\frac{E(2h)}{E(h)})$. Several methods have been proposed for training ODE-nets, such as the adjoint method [10, 35] and the auto-differentiation technique [4]. Since the latter is more stable [21], we use the straightforward auto-differentiation to optimize MSE (mean squared error) loss without any explicit regularization. To circumvent learning loss, We train the neural network sufficiently and test the results near the dataset [29, 31].

We consider two datasets (i) flow data and (ii) random data on domain corresponding to discovery on trajectory and discovery on domain to substantiate our statements, respectively. In particular, we will investigate the results obtained by same HNN model on different domain.

Flow data. The training dataset consists of $I + 1$ data points on a single trajectory starting from x^0 with shared data step T , i.e., x^0, x^1, \dots, x^I where $x^i = \phi_{iT}(x^0)$. These data points are grouped in pairs before being fed into the neural network, denoted as $\mathcal{T} = \{(x^i, x^{i+1})\}_{i=0}^I$. For this type, we define the error between g and \hat{g} by

$$E(g, \hat{g}) = \int_{t \in [0, IT]} \|g(x(t)) - \hat{g}(x(t))\|_{\infty} dt$$

where $x(t) = \phi_t(x^0)$ and compute this error on very fine mesh.

Random data on domain. The training dataset consists grouped pairs of points randomly sampled from the

given domain \mathcal{X} with shared data step T , i.e., $\mathcal{T} = \{(x^i, \phi_T(x^i))\}$ where $x^i \in \mathcal{X}$. For this type, we define the error between g and \hat{g} by

$$E(g, \hat{g}) = \int_{x \in \mathcal{X}} \|g(x) - \hat{g}(x)\|_{\infty} dx,$$

and compute this error by Monte Carlo integration.

5.1 Pendulum problem

We consider the mathematical pendulum of the form

$$\begin{aligned} \frac{d}{dt}p &= -\frac{g}{l} \sin q, \\ \frac{d}{dt}q &= p. \end{aligned}$$

5.1.1 IMDE for ODE-net

To begin with we check out the results for ODE-nets. Here, the chosen numerical methods are the explicit Euler method

$$\Phi_h(y) = y + hf(y),$$

which is of order 1 and the truncation of the IMDE of order 3 is of the form

$$\begin{aligned} f_h^3(y) &= f(y) + \frac{h}{2}f'f(y) + \frac{h^2}{6}f''(f, f)(y) + \frac{h^2}{6}f'f'f(y) \\ &\quad + \frac{h^3}{24}f'''(f, f, f)(y) + \frac{h^3}{8}f''(f'f, f)(y) + \frac{h^3}{24}f'f''(f, f)(y) + \frac{h^3}{24}f'f'f'f(y); \end{aligned}$$

the implicit Euler

$$\Phi_h(y) = y + hf(\Phi_h(y)),$$

which is of order 1 and the truncation of the IMDE of order 3 is of the form

$$\begin{aligned} f_h^3(y) &= f(y) - \frac{h}{2}f'f(y) + \frac{h^2}{6}f''(f, f)(y) + \frac{h^2}{6}f'f'f(y) \\ &\quad - \frac{h^3}{24}f'''(f, f, f)(y) - \frac{h^3}{8}f''(f'f, f)(y) - \frac{h^3}{24}f'f''(f, f)(y) - \frac{h^3}{24}f'f'f'f(y); \end{aligned}$$

and the explicit midpoint rule

$$\Phi_h(y) = y + hf(y + \frac{h}{2}f(y)),$$

which is of order 2 and the truncation of the IMDE of order 3 is given as

$$f_h^3(y) = f(y) + \frac{h^2}{6}f'f'f(y) + \frac{h^2}{24}f''(f, f)(y) - \frac{h^3}{16}f'f''(f, f)(y) - \frac{h^3}{8}f'f'f'f(y).$$

We set $m = l = 1, g = 10$. Neural networks employed are all two hidden layer and 128 neurons. The activation function is chosen to be tanh. We use Adam optimization [33] where the learning rate is set to decay exponentially with linearly decreasing powers from 10^{-2} to 10^{-5} . Results are collected after 3×10^5 parameter updates in ODE-net framework For Euler and explicit midpoint methods while in LMNet framework for implicit Euler.

We first sample flow data on a single trajectory from $t = 0$ to $t = 4$ with data step T and initial condition $y_0 = (0, 1)$. After training, we record the error in Figure 1 top for different data step T (with one composition thus $h = T$) and bottom for different composition number S (with $T = 0.12$ thus $h = 0.12/S$). The error between f and trained f_{net} with respect to h increase linearly for Euler while superlinearly for explicit midpoint, more precisely, the convergence order is 1.03 for Euler while 2.02 for explicit midpoint.

Meanwhile, in Figure 1, the error markedly decreases with the increasing of the truncation order. We also depict the trajectories starting at $(0, 0)$ in the first row of Figure 2, where the learned dynamical system capture the evolution of IMDEs. The second row of Figure 2 show the performance when the data is randomly sampled from space $[-3.8, 3.8] \times [-1.2, 1.2]$. Here, the learned dynamical system coincide with the IMDE more accurately since sufficient data lead to better generalization. These results demonstrate that training ODE-net returns approximations of the IMDE, which are consistent with the theoretical findings.

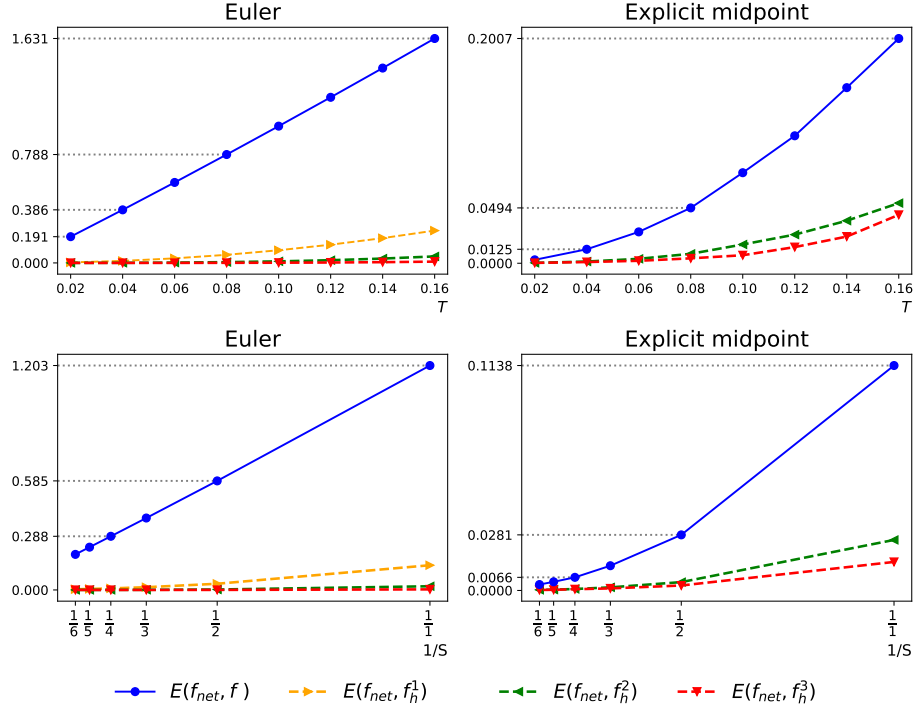


Figure 1: **Error versus h for pendulum problem using flow data.** (Top row) Composition number S is fixed to 1 thus $h = T$. (Bottom row) Data step T is fixed to 0.12 thus $h = 0.12/S$.

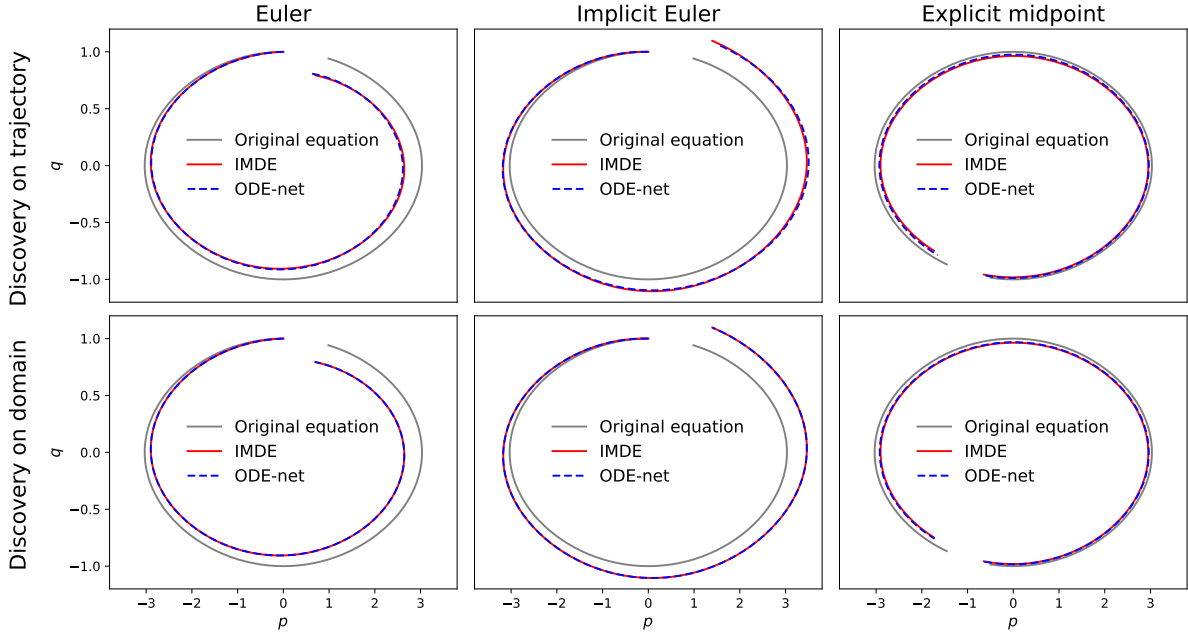


Figure 2: **Pendulum problem.** Phase portraits starting at $(0, 1)$ from $t = 0$ to $t = 2$ for Euler and Implicit Euler while from $t = 1$ to $t = 3$ for explicit midpoint. Composition number is fixed to 1 and data step size is 0.02 for Euler and implicit Euler while 0.12 for explicit midpoint rule.

5.1.2 IMDE for HNN

The pendulum is a Hamiltonian system having the Hamiltonian

$$H(p, q) = \frac{1}{2}p^2 - \frac{g}{l} \cos q,$$

and we also verify the assertion for HNN using this model. This time, we set $l = m = g = 1$, $T = 0.1$ and randomly sample training data with number 6000 from Space 1, $[-1.1, \frac{\pi}{2}] \times [-1.1, \frac{\pi}{2}]$, or Space 2, $[-\frac{\pi}{2}, 1.1] \times [-\frac{\pi}{2}, 1.1]$. This data distribution is demonstrated in the top-left of Figure 3. Test data is generated in the same way with number of 100. Neural network architecture employed in HNN is same as above. Results are collected after 5×10^5 parameter updates using Adam optimization with learning rate 1×10^{-3} . The chosen integrator is the explicit Euler method for NS-HNN and the symplectic Euler method for S-HNN. The symplectic Euler method is given by

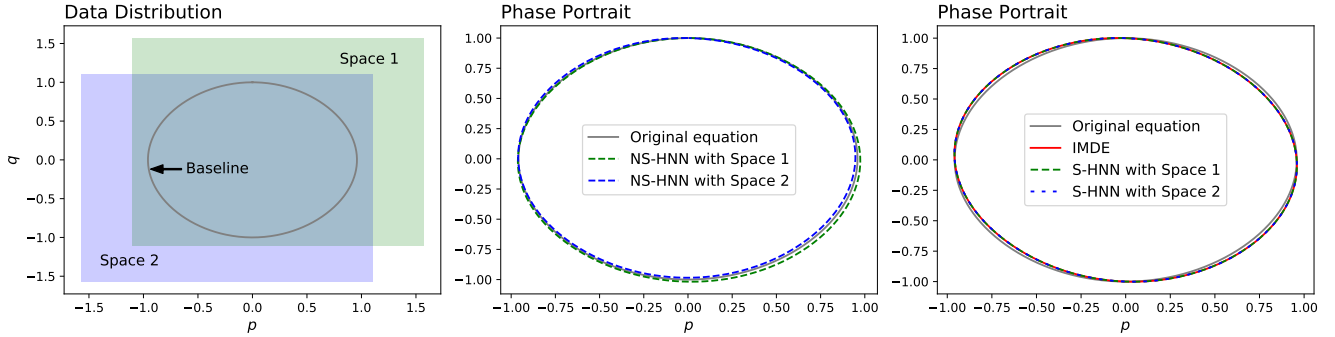


Figure 3: **Pendulum system.** (Left) Data distribution. (Middle) phase portrait for HNN with non-symplectic integrators. (Right) phase portrait for HNN with symplectic integrators.

Integrator	Space	Training loss	Test loss
Explicit Euler	1	8.19×10^{-6}	8.09×10^{-6}
Explicit Euler	2	8.18×10^{-6}	7.98×10^{-6}
Symplectic Euler	1	1.39×10^{-10}	1.68×10^{-10}
Symplectic Euler	2	1.38×10^{-10}	1.25×10^{-10}

Table 2: Training loss and test loss of HNN.

$$\begin{aligned}\bar{p} &= p - h \frac{\partial H(\bar{p}, q)}{\partial q}, \\ \bar{q} &= q + h \frac{\partial H(\bar{p}, q)}{\partial p},\end{aligned}$$

which is symplectic and of order 1, $\Phi_h(p, q) = (\bar{p}, \bar{q})$. The truncation of the IMDE of order 2 is a Hamiltonian system, having the Hamiltonian

$$\begin{aligned}H_h^2(p, q) &= H(p, q) + \frac{h}{2} \frac{\partial H}{\partial p} \frac{\partial H}{\partial q}(p, q) \\ &+ \frac{h^2}{6} \frac{\partial^2 H}{\partial p^2} \left(\frac{\partial H}{\partial q}, \frac{\partial H}{\partial q} \right)(p, q) + \frac{h^2}{6} \frac{\partial^2 H}{\partial p \partial q} \left(\frac{\partial H}{\partial p}, \frac{\partial H}{\partial q} \right)(p, q) + \frac{h^2}{6} \frac{\partial^2 H}{\partial q^2} \left(\frac{\partial H}{\partial p}, \frac{\partial H}{\partial p} \right)(p, q).\end{aligned}$$

Since symplectic integrator is implicit in general, we train it like LMNet, i.e., optimizing

$$\frac{1}{I} \sum_{i=1}^I \left\| p_i - h \frac{\partial u(\bar{p}_i, q_i)}{\partial q} - \bar{p}_i \right\|_2^2 + \left\| q_i + h \frac{\partial u(\bar{p}_i, q_i)}{\partial p} - \bar{q}_i \right\|_2^2,$$

where $(\bar{p}_i, \bar{q}_i) = \phi_h(p, q)$ and u is neural networks.

After training, we solve the exact solutions using initial condition $y_0 = (0, 1)$ in one period. Figure 3 shows the exact dynamics of original equation, IMDE and the equations learned by HNN. Both S-HNN reproduce the phase flow of the same IMDE despite different spaces, while NS-HNN with different data yield discrepant results. Table 2 shows the training loss and test loss of HNN. S-HNN achieves lower loss. Clearly, the numerical results support the assertion.

5.2 Damped oscillator problem

In addition, we consider the two-dimensional damped harmonic oscillator with cubic dynamics, which is also investigated in [32, 38]. The equation is of the form

$$\begin{aligned}\frac{d}{dt}p &= -0.1p^3 + 2.0q^3, \\ \frac{d}{dt}q &= -2.0p^3 - 0.1q^3.\end{aligned}$$

Training data is $\mathcal{T} = \{(y_i, \phi_T(y_i))\}_{i=1}^{10000}$, where $y_i = (p_i, q_i)$ are randomly collected from compact set $[-2.2, 2.2] \times [-2.2, 2.2]$, $\phi_T(y)$ is the exact solution and T is the data step. Meanwhile, test data is generated in the same way with number of 100. Neural network employed is of one hidden layer and 128 neurons with sigmoid activation. We use batch size of 2000 data points and Adam optimization [33] with learning rate $= 1 \times 10^{-4}$. Results are collected after 5×10^5 parameter updates.

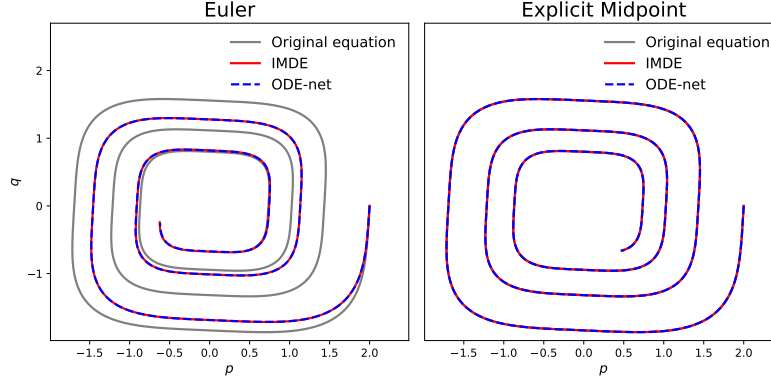


Figure 4: **Damped harmonic oscillator.** **(Left)** The ODE solver is two compositions of explicit Euler method. **(Right)** The ODE solver is two compositions of explicit midpoint rule.

DS	CN	Damped oscillator with Euler method					Lorenz system with explicit midpoint rule				
		Training loss	Test loss	$E(f_{net}, f_h^3)$	$E(f_{net}, f)$	Order	Training loss	$E(f_{net}, f_h^3)$	$E(f_{net}, f)$	Order	
0.01	2	1.28×10^{-9}	1.26×10^{-9}	3.69×10^{-3}	0.139	—	1.47×10^{-9}	4.79×10^{-3}	7.87×10^{-3}	—	
0.02	2	5.22×10^{-9}	3.41×10^{-9}	3.78×10^{-3}	0.277	0.992	4.78×10^{-9}	4.62×10^{-3}	2.30×10^{-2}	1.55	
0.04	2	2.31×10^{-8}	1.74×10^{-8}	5.48×10^{-3}	0.547	0.982	1.35×10^{-8}	1.16×10^{-2}	8.53×10^{-2}	1.89	
0.08	2	1.38×10^{-7}	1.43×10^{-7}	3.70×10^{-2}	1.054	0.947	4.60×10^{-7}	1.18×10^{-1}	3.08×10^{-1}	1.85	
0.04	8	7.60×10^{-9}	6.55×10^{-9}	2.95×10^{-3}	0.139	—	1.31×10^{-8}	4.71×10^{-3}	7.81×10^{-3}	—	
0.04	4	9.60×10^{-9}	1.22×10^{-8}	3.28×10^{-3}	0.276	0.993	1.14×10^{-8}	4.60×10^{-3}	2.29×10^{-2}	1.55	
0.04	2	2.31×10^{-8}	1.74×10^{-8}	5.48×10^{-3}	0.547	0.987	1.35×10^{-8}	1.16×10^{-2}	8.53×10^{-2}	1.89	
0.04	1	5.39×10^{-8}	1.37×10^{-7}	3.71×10^{-2}	1.056	0.949	1.61×10^{-8}	1.16×10^{-1}	3.06×10^{-1}	1.84	

Table 3: **Quantitative results.** DS and IN stand for data step T and composition number S , respectively.

After training, we solve the exact solutions from $t = 0$ to $t = 10$ using initial condition $y_0 = (2, 0)$. Figure 4 shows the exact dynamics of original equation, IMDEs and the equations learned by ODE-nets. Here, the data step is 0.04. The ODE-net accurately capture the evolution of IMDEs. Note that the original equation and the IMDE in the second row coincide due to the high order integrator.

The quantitative results for the explicit Euler method are recorded in Table 3 left side. Here, $E(\cdot, \cdot)$ is calculated by sampling 1×10^6 points from $[-2.2, 2.2] \times [-2.2, 2]$. $E(f_{net}, f_h^3)$ is much less than $E(f_{net}, f)$, which again indicates the approximation target is the IMDE. In addition, the order of $E(f_{net}, f)$ with respect to discrete step is approximately 1, coinciding with Theorem 7.

5.3 Lorenz system

Subsequently, consider the nonlinear Lorenz system

$$\begin{aligned}\frac{d}{dt}p &= 10(q - p), \\ \frac{d}{dt}q &= p(28 - 10r) - q, \\ \frac{d}{dt}r &= 10pq - \frac{8}{3}r,\end{aligned}$$

where $y = (p, q, r)$. The training data consists of data points on a single trajectory from $t = 0$ to $t = 10$ with data step T and initial condition $y_0 = (-0.8, 0.7, 2.6)$. The chosen model architecture and hyper-parameters are the same as in subsection 5.2 except batch size is 500.

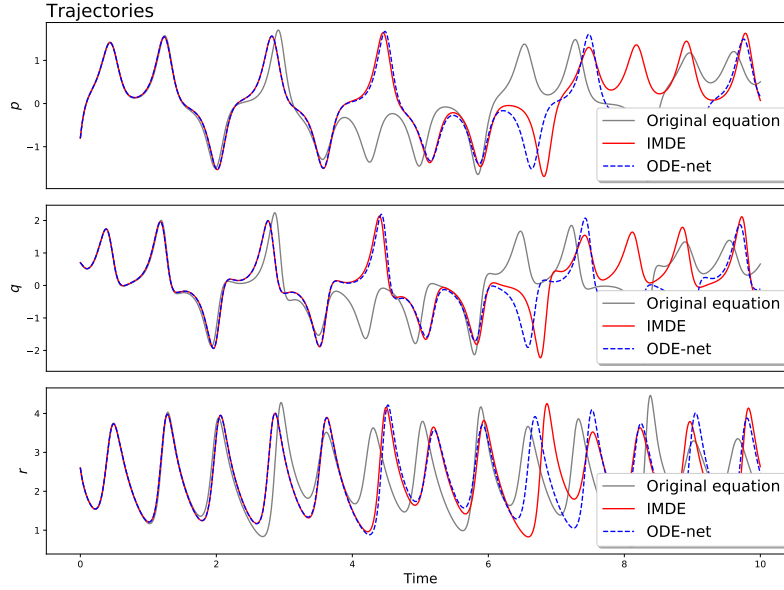


Figure 5: **Lorenz system.** The trajectories of original equation also represent the training data.

Upon training the ODE-net, we solve the exact solution from $t = 0$ to $t = 10$ using initial condition $y_0 = (-0.8, 0.7, 2.6)$. Figure 5 depicts the exact trajectories of original equation, IMDE and the equation learned by ODE-net. Here, the data step is 0.04 and the ODE solver is two compositions of explicit midpoint rule. These results could be illuminated by the theoretical findings of this paper. To begin with, the identified system accurately reproduces the trajectories of the IMDE from $t = 0$ to $t = 4$ due to the generalization ability of neural networks. Then, the ODE-net tries to capture the dynamics of the IMDE, however, there are no sufficient information tell how ϕ_T acts later. Thus the discrepancies between the trajectories of the IMDE and the training data explode over time, as demonstrated in Figure 5, the trajectories of the IMDE significantly deviate from the original equation at around $t = 4$. Consequently, the identified system drifts away after $t = 4$ as errors accumulate.

The quantitative results are recorded in Table 3 right side. Here, $E(f_{net}, f_h^3)$ is less than $E(f_{net}, f)$ and the order of $E(f_{net}, f)$ with respect to discrete step is approximately 2, which are consistent with the theoretical findings.

6 Summary

In this paper, we perform the numerical analysis of discovery of dynamics using ODE based models. Training an ODE-net returns an approximation of the inverse modified differential equation (IMDE). In addition, the convergence analysis of data-driven discovery using ODE-net is presented, which shown that the error between trained network f_{net} and the unknown vector field f is bounded by the sum of discrete error Ch^p and learning loss, where h is the discrete step size and p is the order of integrator. We also discuss learning Hamiltonian system, and demonstrate that both ODE-net using non-symplectic integrators and LMNet tend not to learn conservation laws theoretically. IMDEs make clear the behavior of HNN and reveal the potential issue. Finally, numerical results support the theoretical analysis.

One limitation of our work is the generalization and analyticity requirement on complex space. Quantifying the generalization errors and implicit regularization for supervised learning is still an open research problem. Whereas we observe excellent performance in experiments, we would like to further investigate such issue for ODE-net in the future.

Low frequency and fine step are essential for both theory and practice. For discovery high frequencies dynamics, we are inevitably faced with choosing specific ODE solver employed in ODE-net. One possible approach is filtered integrator or the Modulated Fourier Expansion [26].

Approximation targets depend on the ODE solver. As HNN needs symplectic integrator, further numerical analysis are needed. It is another interesting problem.

A Proof of Theorem 4

Proof. The computation procedure of f_h uniquely defines the functions f_k and can be rewritten as the following recursion:

$$f_k = \lim_{h \rightarrow 0} \frac{\phi_{h,f} - \Phi_{h,f_h^{k-1}}}{h^{k+1}}. \quad (15)$$

We first prove

$$f_k = \lim_{h \rightarrow 0} \frac{\phi_{Sh,f} - \left(\Phi_{h,f_h^{k-1}}\right)^S}{Sh^{k+1}}, \quad (16)$$

by induction on $S \geq 1$. First, the case when $S = 1$ is obvious. Suppose now that the statement holds for $S - 1$. Then, by this inductive hypothesis, we obtain

$$\begin{aligned} \phi_{Sh,f} - \left(\Phi_{h,f_h^{k-1}}\right)^S &= \left(\phi_{h,f} - \Phi_{h,f_h^{k-1}}\right) \circ \phi_{(S-1)h,f} + \Phi_{h,f_h^{k-1}} \circ \left(\phi_{(S-1)h,f} - \left(\Phi_{h,f_h^{k-1}}\right)^{S-1}\right) \\ &= h^{k+1} f_k \circ \phi_{(S-1)h,f} + (S-1)h^{k+1} \Phi_{h,f_h^{k-1}} \circ f_k + O(h^{k+2}) \\ &= Sh^{k+1} f_k + O(h^{k+2}), \end{aligned}$$

where we have used the fact that $\phi_{(S-1)h,f} = I_N + O((S-1)h)$ and $\Phi_{h,f_h^{k-1}} = I_N + O(h)$. Hence the induction is completed.

Suppose that the vector field of IMDE for $(\Phi_h)^S$ is of the form $F_{Sh}(y) = \sum_{k=0}^{\infty} (Sh)^k F_k(y)$. We next prove that $S^k F_k = f_k$ by induction on k . First the case when $k = 0$ is obvious since $F_0 = f_0 = f$. Suppose now $S^k F_k = f_k$ holds for $k \leq K - 1$. This inductive hypothesis implies that $F_{Sh}^{K-1} = f_h^{K-1}$. Using (15) for F_K we obtain

$$F_K = \lim_{h \rightarrow 0} \frac{\phi_{Sh,f} - \left(\Phi_{h,F_{Sh}^{K-1}}\right)^S}{(Sh)^{K+1}}.$$

This together with (16) concludes the induction and thus completes the proof. \square

B Proof of Theorem 5

Proof. The approach for computation of f_h is presented in two steps. To begin with, by setting $t = mh$ and $F(y) = I_N(y)$ in the formula (5), the left of (11) can be expanded as

$$\begin{aligned} \sum_{m=0}^M \alpha_m \phi_{mh,f}(x) &= \sum_{m=0}^M \alpha_m \sum_{k=0}^{\infty} \frac{(mh)^k}{k!} (D^k I_N)(x) \\ &= \sum_{k=0}^{\infty} h^k \left[\sum_{m=0}^M \alpha_m \frac{m^k}{k!} (D^k I_N)(x) \right]. \end{aligned} \quad (17)$$

In addition, using the formula (5) with setting $t = mh$ and $F(y) = f_h(y)$ implies

$$h \sum_{m=0}^M \beta_m f_h(\phi_{mh,f}(x)) = h \sum_{m=0}^M \beta_m \sum_{j=0}^{\infty} \frac{(mh)^j}{j!} \sum_{i=0}^{\infty} h^i (D^j f_i)(x)$$

Interchanging the summation order, we obtain

$$\begin{aligned} h \sum_{m=0}^M \beta_m f_h(\phi_{mh,f}(x)) &= h \sum_{m=0}^M \beta_m \sum_{k=0}^{\infty} h^k \sum_{j=0}^k \frac{m^j}{j!} (D^j f_{k-j})(x) \\ &= \sum_{k=0}^{\infty} h^{k+1} \sum_{m=0}^M \beta_m [f_k(x) + \sum_{j=1}^k \frac{m^j}{j!} (D^j f_{k-j})(x)]. \end{aligned} \quad (18)$$

Comparing coefficients of h^k in the expression (17) and (18) for $k = 0, 1, 2, \dots$ yields

$$\sum_{m=0}^M \alpha_m = 0,$$

the consistency condition, and

$$\sum_{m=0}^M \beta_m [f_k(x) + \sum_{j=1}^k \frac{m^j}{j!} (D^j f_{k-j})(x)] = \sum_{m=0}^M \alpha_m \frac{m^{k+1}}{(k+1)!} (D^{k+1} I_N)(x).$$

By plugging $(D^{k+1} I_N)(x) = (D^k f)(x)$ and setting $y := x$, unique f_k are obtained recursively, i.e.,

$$f_k(y) = \frac{1}{(\sum_{m=0}^M \beta_m)} \sum_{m=0}^M \alpha_m \frac{m^{k+1}}{(k+1)!} (D^k f)(y) - \frac{1}{(\sum_{m=0}^M \beta_m)} \sum_{m=0}^M \beta_m \sum_{j=1}^k \frac{m^j}{j!} (D^j f_{k-j})(y).$$

Here, the right expression only involves f_j with $j < k$ and

$$\sum_{m=0}^M \beta_m = \sum_{m=0}^M m \alpha_m \neq 0$$

for weakly stable and consistent methods. □

C proof of Theorem 6

Proof. For a Hamiltonian system (4), the target function f obeys $f(y) = J^{-1} \nabla H(y)$. which yields $f_0 = J^{-1} \nabla H(y)$. Assume $f_k(y) = J^{-1} \nabla H_k(y)$ for $k = 1, 2, \dots, K$, we need to prove the existence of $H_{K+1}(y)$ satisfying

$$f_{K+1}(y) = J^{-1} \nabla H_{K+1}(y).$$

By induction, the truncated IMDE

$$\frac{d}{dt}\tilde{y} = f_h^K(\tilde{y}) = f(\tilde{y}) + hf_1(\tilde{y}) + h^2f_2(\tilde{y}) + \cdots + h^Kf_K(\tilde{y})$$

has the Hamiltonian $H(\tilde{y}) + hH_1(\tilde{y}) + \cdots + h^KH_K(\tilde{y})$. For arbitrary initial value x , the numerical solution $\Phi_{h,f_h^K}(x)$ satisfies

$$\phi_{h,f}(x) = \Phi_{h,f_h^K}(x) + h^{K+2}f_{K+1}(x) + O(h^{K+3}).$$

And thus

$$\phi'_{h,f}(x) = \Phi'_{h,f_h^K}(x) + h^{K+2}f'_{K+1}(x) + O(h^{K+3}),$$

where $\phi_{h,f}$ and Φ_{h,f_h^K} are symplectic maps, and $\Phi'_{h,f_h^K}(y) = I + O(h)$. Then, we have

$$J = \phi'_{h,f}(x)^T J \phi'_{h,f}(x) = J + h^{K+2}(f'_{K+1}(x)^T J + J f'_{K+1}(y)) + O(h^{K+3}).$$

Consequently, $f'_{K+1}(x)^T J + J f'_{K+1}(x) = 0$, i.e., $J f'_{K+1}(x)$ is symmetric. According to the Integrability Lemma [27, Lemma VI.2.7], for any x , there exists a neighbourhood and a smooth function H_{K+1} obeying

$$f_{K+1}(x) = J^{-1} \nabla H_{K+1}(x)$$

on this neighbourhood. Hence the induction holds and the proof is completed \square

D Proof of Theorem 7

D.1 Properties of Runge-Kutta methods

To prove Theorem 7, we firstly demonstrate that the condition (14) is satisfied for Runge-Kutta methods (2). Similar statements holds for partitioned Runge-Kutta methods.

Lemma 1. *For a Runge-Kutta method (2) denoted as Φ_h , let*

$$\mu = \sum_{i=1}^s |b_i|, \quad \kappa = \max_{1 \leq i \leq s} \sum_{j=1}^s |a_{ij}|.$$

Consider g, \hat{g} satisfying $\|g\|_{\mathcal{B}(\mathcal{K}, r)} \leq m, \|\hat{g}\|_{\mathcal{B}(\mathcal{K}, r)} \leq m$, if $\kappa \neq 0$, then $\Phi_{h,g}, \Phi_{h,\hat{g}}$ are analytic for $|h| \leq h_0 = r/4\kappa m$ and

$$\|\Phi_{h,\hat{g}} - \Phi_{h,g}\|_{\mathcal{K}} \leq 2\mu|h| \|\hat{g} - g\|_{\mathcal{B}(\mathcal{K}, |h|\kappa m)}.$$

Furthermore,

$$\|\hat{g} - g\|_{\mathcal{K}} \leq \frac{1}{|h|} \|\Phi_{h,\hat{g}}(y) - \Phi_{h,g}(y)\|_{\mathcal{K}} + 2\mu \frac{|h|}{h_0 - |h|} \|\hat{g} - g\|_{\mathcal{B}(\mathcal{K}, |h|\kappa m)}.$$

Proof. For $y \in \mathcal{B}(\mathcal{K}, r/2)$ and $\|\Delta y\| \leq 1$, the function $\alpha(z) = f(y + z\Delta y)$ is analytic for $|z| \leq r/2$ and bounded by m . By Cauchy's estimate, we obtain

$$\|f'(y)\Delta y\| = \|\alpha'(0)\| \leq 2m/r,$$

and $\|f'(y)\| \leq 2m/r$ for $y \in \mathcal{B}(\mathcal{K}, r/2)$ in the operator norm.

For a Runge-Kutta method (2) with initial point y_0 , the solution can be obtained by the nonlinear systems

$$\begin{aligned} u_i &= y_0 + h \sum_{j=1}^s a_{ij} \hat{g}(u_j) \quad i = 1, \dots, s. & \Phi_{h,\hat{g}}(y_0) &= y_0 + h \sum_{i=1}^s b_i \hat{g}(u_i), \\ v_i &= y_0 + h \sum_{j=1}^s a_{ij} g(v_j) \quad i = 1, \dots, s. & \Phi_{h,g}(y_0) &= y_0 + h \sum_{i=1}^s b_i g(v_i), \end{aligned}$$

Here, $y_0 \in \mathcal{K}$. Due to the Implicit Function Theorem [44], u_i, v_i possess unique solution on the closed set $\mathcal{B}(\mathcal{K}, |h|\kappa m)$ if $2|h|\kappa m/r \leq \gamma < 1$ and the method is analytic for $|h| \leq \gamma r/2\kappa m$.

In addition,

$$\begin{aligned} \max_{1 \leq i \leq s} \|u_i - v_i\| &\leq |h| \sum_{j=1}^s |a_{ij}| \|\hat{g}(u_j) - \hat{g}(v_j)\| + |h| \sum_{j=1}^s |a_{ij}| \|\hat{g}(v_j) - g(v_j)\| \\ &\leq |h| \kappa \frac{2m}{r} \max_{1 \leq j \leq s} \|u_j - v_j\| + |h| \kappa \|\hat{g} - g\|_{\mathcal{B}(\mathcal{K}, |h| \kappa m)}. \end{aligned}$$

Thus we obtain

$$\max_{1 \leq i \leq s} \|u_i - v_i\| \leq \frac{\kappa}{1 - |h| \kappa \frac{2m}{r}} |h| \|\hat{g} - g\|_{\mathcal{B}(\mathcal{K}, |h| \kappa m)}.$$

Next, we have

$$\begin{aligned} \|\Phi_{h, \hat{g}}(y_0) - \Phi_{h, g}(y_0)\| &\leq |h| \sum_{i=1}^s |b_i| \|\hat{g}(u_i) - \hat{g}(v_i)\| + |h| \sum_{i=1}^s |b_i| \|\hat{g}(v_i) - g(v_i)\| \\ &\leq |h| \mu \frac{2m}{r} \max_{1 \leq j \leq s} \|u_j - v_j\| + |h| \mu \|\hat{g} - g\|_{\mathcal{B}(\mathcal{K}, |h| \kappa m)} \\ &\leq \left(|h| \mu \frac{2m}{r} \frac{\kappa}{1 - |h| \kappa \frac{2m}{r}} + \mu \right) |h| \|\hat{g} - g\|_{\mathcal{B}(\mathcal{K}, |h| \kappa m)}. \end{aligned}$$

Taking $\gamma = 1/2$, together with the arbitrariness of y_0 , yields

$$\|\Phi_{h, \hat{g}} - \Phi_{h, g}\|_{\mathcal{K}} \leq 2\mu |h| \|\hat{g} - g\|_{\mathcal{B}(\mathcal{K}, |h| \kappa m)}.$$

These complete the first part of the proof.

Finally, using Cauchy's estimate, we deduce that

$$\left\| \frac{d^i}{dh^i} (\Phi_{h, \hat{g}}(y_0) - \Phi_{h, g}(y_0)) \Big|_{h=0} \right\| \leq i! 2\mu \|\hat{g} - g\|_{\mathcal{B}(\mathcal{K}, |h| \kappa m)} \left(\frac{1}{h_0} \right)^{i-1}.$$

The analyticity also implies

$$\Phi_{h, \hat{g}}(y_0) - \Phi_{h, g}(y_0) = \sum_{i=1}^{\infty} \frac{h^i}{i!} \frac{d^i}{dh^i} (\Phi_{h, \hat{g}}(y_0) - \Phi_{h, g}(y_0)) \Big|_{h=0}.$$

By triangle inequality, we obtain

$$\begin{aligned} \|\Phi_{h, \hat{g}}(y_0) - \Phi_{h, g}(y_0)\| &\geq |h| \|\hat{g}(y_0) - g(y_0)\| - \sum_{i=2}^{\infty} \left\| \frac{h^i}{i!} \frac{d^i}{dh^i} (\Phi_{h, \hat{g}}(y_0) - \Phi_{h, g}(y_0)) \Big|_{h=0} \right\| \\ &\geq |h| \|\hat{g}(y_0) - g(y_0)\| - 2\mu |h| \|\hat{g} - g\|_{\mathcal{B}(\mathcal{K}, |h| \kappa m)} \sum_{i=2}^{\infty} \left(\frac{|h|}{h_0} \right)^{i-1}. \end{aligned}$$

Therefore,

$$\|\hat{g} - g\|_{\mathcal{K}} \leq \frac{1}{|h|} \|\Phi_{h, \hat{g}} - \Phi_{h, g}\|_{\mathcal{K}} + 2\mu \frac{|h|}{h_0 - |h|} \|\hat{g} - g\|_{\mathcal{B}(\mathcal{K}, |h| \kappa m)},$$

which concludes the proof. \square

D.2 Choice of K and estimation of truncation

As aforementioned, The series in (8) does not converge in general and need to be truncated. There have been many rigorous estimates for conventional modified equations [5, 24, 25, 40], which inspire us to complete the proofs. In particular, we employ the induction idea in [40] for IMDE scenario below.

Lemma 2. Let $f(y)$ be analytic in $\mathcal{B}(\mathcal{K}, r)$ and satisfy $\|f\|_{\mathcal{B}(\mathcal{K}, r)} \leq m$. Suppose the integrator Φ_h of order p satisfies condition (14). Take $\eta = \max\{6, \frac{b_2+1}{29} + 1\}$, $\zeta = 10(\eta - 1)$, $q = -\ln(2b_2)/\ln 0.912$ and K equals to the largest integer satisfying

$$\frac{\zeta(K - p + 2)^q |h|m}{\eta r} \leq e^{-q}.$$

If $|h|$ is small enough such that $K \geq p$, then the truncated IMDE satisfies

$$\begin{aligned} \|\Phi_{h, f_h^K} - \phi_{h, f}\|_{\mathcal{K}} &\leq b_2 \eta m e^{2q - qp} |h| e^{-\gamma/|h|^{1/q}}, \\ \|f_h^K - f\|_{\mathcal{K}} &\leq b_2 \eta m \left(\frac{\zeta m}{b_1 r}\right)^p (1 + 1.38^q d_p) |h|^p, \\ \|f_h^K\|_{\mathcal{K}} &\leq (\eta - 1)m, \end{aligned}$$

where $\gamma = \frac{q}{e} \left(\frac{b_1 r}{\zeta m}\right)^{1/q}$, $d_p = p^{qp} e^{-q(p-1)}$.

Proof. For $0 \leq \alpha < 1$ and $|h| \leq h_0 = b_1(1 - \alpha)r/m$, the condition (14), together with the fact that $\mathcal{B}(\mathcal{B}(\mathcal{K}, \alpha r), (1 - \alpha)r) = \mathcal{B}(\mathcal{K}, r)$ implies

$$\begin{aligned} \|\Phi_{h, f} - \phi_{h, f}\|_{\mathcal{B}(\mathcal{K}, \alpha r)} &\leq \|\Phi_{h, f} - I_N\|_{\mathcal{B}(\mathcal{K}, \alpha r)} + \|\phi_{h, f} - I_N\|_{\mathcal{B}(\mathcal{K}, \alpha r)} \\ &\leq (b_2 + 1)|h|m \leq b_1(b_2 + 1)(1 - \alpha)r \end{aligned}$$

Here, the map $\Phi_{h, f} - \phi_{h, f}$ contains the factor h^{p+1} since $\Phi_{h, f}$ is of order p . By the maximum principle for analytic functions [44], we obtain

$$\left\| \frac{\Phi_{h, f} - \phi_{h, f}}{h^{p+1}} \right\|_{\mathcal{B}(\mathcal{K}, \alpha r)} \leq \frac{b_1(b_2 + 1)(1 - \alpha)r}{h_0^{p+1}}$$

and thus (since (15))

$$\|f_p\|_{\mathcal{B}(\mathcal{K}, \alpha r)} \leq \frac{b_1(b_2 + 1)(1 - \alpha)r}{h_0^{p+1}} = (b_2 + 1)m \left(\frac{m}{b_1(1 - \alpha)r}\right)^p. \quad (19)$$

Below we proceed to prove that for $\alpha \in [0, 1]$, if

$$|h| \leq h_k := \frac{b_1(1 - \alpha)r}{\zeta(k - p + 1)^q m},$$

then

$$\|f_k\|_{\mathcal{B}(\mathcal{K}, \alpha r)} \leq b_2 \eta m \left(\frac{\zeta(k - p + 1)^q m}{b_1(1 - \alpha)r}\right)^k \quad (20)$$

for $k \geq p$ by induction, where $\eta = \max\{6, \frac{b_2+1}{29} + 1\}$, $\zeta = 10(\eta - 1)$ and $q = -\ln(2b_2)/\ln 0.912$. First, the case when $k = p$ is obvious since (19). Suppose now (20) holds for $k \leq K$. If $|h| \leq h_{K+1}$, taking

$$\delta_{K+1} := \frac{\eta - 1}{(K - p + 2)^q \zeta}, \quad \beta_K := (1 - \delta_{K+1})(K - p + 2)^q$$

yields that for $p \leq k \leq K$

$$|h| \leq \frac{b_1(1 - \alpha)r}{\zeta(K - p + 2)^q m} \leq \frac{b_1(1 - \alpha - \delta_{K+1}(1 - \alpha))r}{\zeta(k - p + 1)^q m}.$$

Therefore, by inductive hypothesis we obtain

$$\|f_k\|_{\mathcal{B}(\mathcal{K}, (\alpha + \delta_{K+1}(1 - \alpha))r)} \leq b_2 \eta m \left(\frac{\zeta(k - p + 1)^q m}{b_1(1 - \delta_{K+1})(1 - \alpha)r}\right)^k$$

via replacing the parameter α by $\alpha + \delta_{K+1}(1 - \alpha) \in [\delta_{K+1}, 1]$ in (20). This indicates

$$\|f_h^K\|_{\mathcal{B}(\mathcal{K}, (\alpha + \delta_{K+1}(1 - \alpha))r)} \leq m \left[1 + (b_2 + 1) \left(\frac{1}{\zeta \beta_K}\right)^p + b_2 \eta \sum_{k=p+1}^K \left(\frac{(k - p + 1)^q}{\beta_K}\right)^k \right].$$

Observe that

$$\sum_{k=p+1}^K \left(\frac{(k-p+1)}{(K-p+1.9)} \right)^k \leq 0.912,$$

which is maximal for $K = 6$ and $p = 1$, and

$$\sum_{k=p+1}^K \left(\frac{(k-p+1)^q}{\beta_K} \right)^k \leq \left[\sum_{k=p+1}^K \left(\frac{(k-p+1)}{(K-p+1.9)} \right)^k \right]^q,$$

we deduce that

$$\|f_h^K\|_{\mathcal{B}(\mathcal{K}, (\alpha + \delta_{K+1}(1-\alpha))r)} \leq (\eta - 1)m. \quad (21)$$

Here, we have used the definition of η , ζ and q . Subsequently, by this estimate and condition (14), we obtain

$$\|\Phi_{h, f_h^K} - I_N\|_{\mathcal{B}(\mathcal{K}, \alpha r)} \leq |h|b_2 \|f_h^K\|_{\mathcal{B}(\mathcal{K}, (\alpha + \delta_{K+1}(1-\alpha))r)} \leq |h|b_2(\eta - 1)m,$$

where

$$|h| \leq \frac{b_1(1-\alpha)r}{\zeta(K-p+2)^q m} = \frac{b_1\delta_{K+1}(1-\alpha)r}{(\eta - 1)m}.$$

And then using triangle inequality yields

$$\|\Phi_{h, f_h^K} - \phi_{h, f}\|_{\mathcal{B}(\mathcal{K}, \alpha r)} \leq \|\Phi_{h, f_h^K} - I_N\|_{\mathcal{B}(\mathcal{K}, \alpha r)} + \|\phi_{h, f} - I_N\|_{\mathcal{B}(\mathcal{K}, \alpha r)} \leq h_K b_2 \eta m.$$

Again by the maximum principle for analytic functions, together with the fact that $\Phi_{h, f_h^K} - \phi_{h, f}$ contains the factor h^{K+2} , we deduce that

$$\left\| \frac{\Phi_{h, f_h^K} - \phi_{h, f}}{h^{K+2}} \right\|_{\mathcal{B}(\mathcal{K}, \alpha r)} \leq \frac{h_K b_2 \eta m}{h_K^{K+2}}. \quad (22)$$

Again by (15), we conclude that

$$\|f_{K+1}\|_{\mathcal{B}(\mathcal{K}, \alpha r)} \leq b_2 \eta m \left(\frac{\zeta(K-p+2)^q m}{b_1(1-\alpha)r} \right)^{K+1},$$

which complete the induction.

The above induction also shows that (22) holds if $|h| \leq h_{K+1}$. Taking $\alpha = 0$ we have

$$\|\Phi_{h, f_h^K} - \phi_{h, f}\|_{\mathcal{K}} \leq b_2 \eta |h| m \left(\frac{\zeta(K-p+2)^q |h| m}{b_1 r} \right)^{K+1}.$$

We set K^* to be the largest integer satisfying

$$\frac{\zeta(K^* - p + 2)^q |h| m}{b_1 r} \leq e^{-q}.$$

Clearly, $|h| \leq h_{K^*+1}$ with $\alpha = 0$. Therefore,

$$\|\Phi_{h, f_h^{K^*}} - \phi_{h, f}\|_{\mathcal{K}} \leq b_2 \eta |h| m \left(\frac{\zeta(K^* - p + 2)^q |h| m}{b_1 r} \right)^{K^*+1} \leq b_2 \eta m e^{2q - qp} |h| e^{-\gamma/|h|^{1/q}},$$

where $\gamma = \frac{q}{e} \left(\frac{b_1 r}{\zeta m} \right)^{1/q}$. The first part of the lemma has been completed.

Next, according to (20) we obtain

$$\begin{aligned} \|f_h^{K^*} - f\|_{\mathcal{K}} &\leq b_2 \eta m \left(\frac{\zeta |h| m}{b_1 r} \right)^p \left[1 + \sum_{k=p+1}^{K^*} \frac{(k-p+1)^{qp}}{e^{q(k-p)}} \left(\frac{(k-p+1)}{(K^* - p + 2)} \right)^{q(k-p)} \right] \\ &\leq b_2 \eta m \left(\frac{\zeta m}{b_1 r} \right)^p (1 + 1.38^q d_p) |h|^p, \end{aligned}$$

where $d_p = p^{qp} e^{-q(p-1)}$ satisfying $d_p \geq (k-p+1)^{qp} e^{-q(k-p)}$ for any $k \geq p+1$.

Finally, we immediately derive the boundedness of f_h^K due to (21). The proof has been completed. \square

D.3 Error estimation

With Lemma 2, we can obtain error estimation for one-step integrator.

Lemma 3. *For $x \in \mathbb{R}^N$, suppose the analyticity assumptions are satisfied and the integrator Φ_h satisfies condition (14), then, for sufficiently small $h > 0$, there exist integer $K = K(h)$ (as defined in Lemma 2), and constant q, γ, c_1, c_2, C which depend on m, r_1, r_2 and the integrator Φ_h , such that*

$$\begin{aligned}\|f_{net}(x) - f_h^K(x)\| &\leq c_1 e^{-\gamma/h^q} + C\mathcal{L}, \\ \|f_{net}(x) - f(x)\| &\leq c_2 h^p + C\mathcal{L},\end{aligned}$$

where $\mathcal{L} = \|\Phi_{h,f_{net}} - \phi_{h,f}\|_{\mathcal{B}(x,r_1)}/h$.

Proof. According to the first inequality of Lemma 2, there exist K, c, γ, q such that

$$\|\Phi_{h,f_h^K} - \phi_{h,f}\|_{\mathcal{B}(x,r_1)} \leq che^{-\gamma/h^{1/q}},$$

which immediately yields

$$\delta := \frac{1}{h} \|\Phi_{h,f_{net}} - \Phi_{h,f_h^K}\|_{\mathcal{B}(x,r_1)} \leq \mathcal{L} + ce^{-\gamma/h^{1/q}}. \quad (23)$$

Next, by the third inequality of Lemma 2, there exists $M \geq m$ such that $f_h^K < M$. Let

$$h_0 = b_1 r_2 / M, \quad \lambda = b_2 \frac{h}{h_0 - h}.$$

Using the third item of (14), we have

$$\|f_{net} - f_h^K\|_{\mathcal{B}(x,jhb_3M)} \leq \delta + \lambda \|f_{net} - f_h^K\|_{\mathcal{B}(x,(j+1)hb_3M)}$$

for $0 \leq j \leq r_1/hb_3M$. This yields

$$\|f_{net} - f_h^K\|_{\mathcal{B}(x,jhb_3M)} - \frac{\delta}{1-\lambda} \leq \lambda \left(\|f_{net} - f_h^K\|_{\mathcal{B}(x,(j+1)hb_3M)} - \frac{\delta}{1-\lambda} \right).$$

Therefore,

$$\|f_{net}(x) - f_h^K(x)\| \leq \lambda^{r_1/hb_3M} \left(\|f_{net} - f_h^K\|_{\mathcal{B}(x,r_1+hb_3M)} - \frac{\delta}{1-\lambda} \right) + \frac{\delta}{1-\lambda}. \quad (24)$$

Combining (23) and (24) we conclude that

$$\|f_{net}(x) - f_h^K(x)\| \leq c_1 e^{-\gamma/h^{1/q}} + C\mathcal{L},$$

where c_1, C are constants satisfying

$$C \geq 1/(1-\lambda), \quad c_1 \geq C \cdot c + 2Me^{\gamma/h^{1/q}} \lambda^{r_1/b_3M}.$$

By this estimation together with the second inequality in Lemma 2, we obtain the second estimation and complete the proof. \square

With this results, we are able to provide the proof of Theorem 7.

Proof of Theorem 7. Using the fact that several compositions of Runge-Kutta methods are again Runge-Kutta methods, Lemma 1, Lemma 3 and Theorem 4, we conclude the proof. \square

References

- [1] J. Anderson, I. Kevrekidis, and R. Rico-Martinez. A comparison of recurrent training algorithms for time series analysis and system identification. *Computers & chemical engineering*, 20:S751–S756, 1996.
- [2] V. I. Arnold. *Mathematical methods of classical mechanics*, volume 60. Springer Science & Business Media, 2013.
- [3] V. I. Arnold, V. V. Kozlov, and A. I. Neishtadt. *Mathematical aspects of classical and celestial mechanics*, volume 3. Springer Science & Business Media, 2007.
- [4] A. G. Baydin, B. A. Pearlmutter, A. A. Radul, and J. M. Siskind. Automatic differentiation in machine learning: a survey. *The Journal of Machine Learning Research*, 18(1):5595–5637, 2017.
- [5] G. Benettin and A. Giorgilli. On the hamiltonian interpolation of near-to-the identity symplectic mappings with application to symplectic integration algorithms. *Journal of Statistical Physics*, 74(5):1117–1143, 1994.
- [6] T. Bertalan, F. Dietrich, I. Mezić, and I. G. Kevrekidis. On learning hamiltonian systems from data. *Chaos: An Interdisciplinary Journal of Nonlinear Science*, 29(12):121107, 2019.
- [7] S. L. Brunton and J. N. Kutz. *Data-driven science and engineering: Machine learning, dynamical systems, and control*. Cambridge University Press, 2019.
- [8] J. C. Butcher. *The numerical analysis of ordinary differential equations: Runge-Kutta and general linear methods*. Wiley-Interscience, 1987.
- [9] P. Chartier, E. Hairer, and G. Vilmart. Numerical integrators based on modified differential equations. *Mathematics of computation*, 76(260):1941–1953, 2007.
- [10] T. Chen, Y. Rubanova, J. Bettencourt, and D. Duvenaud. Neural ordinary differential equations. In *Advances in Neural Information Processing Systems 31: Annual Conference on Neural Information Processing Systems 2018, NeurIPS 2018, 3-8 December 2018, Montréal, Canada*, pages 6572–6583, 2018.
- [11] Z. Chen, J. Zhang, M. Arjovsky, and L. Bottou. Symplectic recurrent neural networks. In *8th International Conference on Learning Representations, ICLR, Addis Ababa, Ethiopia, April 26-30, 2020*. OpenReview.net, 2020.
- [12] Q. Du, Y. Gu, H. Yang, and C. Zhou. The discovery of dynamics via linear multistep methods and deep learning: Error estimation. *arXiv preprint arXiv:2103.11488*, 2021.
- [13] W. E. A proposal on machine learning via dynamical systems. *Communications in Mathematics and Statistics*, 5(1):1–11, 2017.
- [14] W. E, J. Han, and Q. Li. A mean-field optimal control formulation of deep learning. *Research in the Mathematical Sciences*, 6(1):1–41, 2019.
- [15] T. Eirola. Aspects of backward error analysis of numerical odes. *Journal of Computational and Applied Mathematics*, 45(1-2):65–73, 1993.
- [16] K. Feng. On difference schemes and symplectic geometry. In *Proceedings of the 5th International Symposium on differential geometry and differential equations, August 1984 Beijing, China*, pages 42–58. Science Press, Beijing, 1985.
- [17] K. Feng. Difference schemes for Hamiltonian formalism and symplectic geometry. *Journal of Computational Mathematics*, 4(3):279–289, 1986.
- [18] K. Feng. Formal power series and numerical algorithms for dynamical systems. In *Proceedings of international conference on scientific computation, Hangzhou, China, Series on Appl. Math. Singapore: World Scientific*, volume 1, pages 28–35, 1991.

- [19] K. Feng. Formal dynamical systems and numerical algorithms. *SERIES ON APPLIED MATHEMATICS*, 4:1–10, 1993.
- [20] K. Feng. The step-transition operators for multi-step methods of ODE’s. *Journal of Computational Mathematics*, 16(3):193–202, 1998.
- [21] A. Gholaminejad, K. Keutzer, and G. Biros. ANODE: unconditionally accurate memory-efficient gradients for neural ODEs. In *Proceedings of the Twenty-Eighth International Joint Conference on Artificial Intelligence, IJCAI 2019, Macao, China, August 10-16, 2019*, pages 730–736. ijcai.org, 2019.
- [22] R. González-García, R. Rico-Martínez, and I. G. Kevrekidis. Identification of distributed parameter systems: A neural net based approach. *Computers & chemical engineering*, 22:S965–S968, 1998.
- [23] S. Greydanus, M. Dzamba, and J. Yosinski. Hamiltonian neural networks. In *Advances in Neural Information Processing Systems 32: Annual Conference on Neural Information Processing Systems, NeurIPS, 8-14 December 2019, Vancouver, BC, Canada*, pages 15353–15363, 2019.
- [24] E. Hairer. Backward error analysis for multistep methods. *Numerische Mathematik*, 84(2):199–232, 1999.
- [25] E. Hairer and C. Lubich. The life-span of backward error analysis for numerical integrators. *Numerische Mathematik*, 76(4):441–462, 1997.
- [26] E. Hairer and C. Lubich. Long-time energy conservation of numerical methods for oscillatory differential equations. *SIAM Journal on Numerical Analysis*, 38(2):414–441, 2001.
- [27] E. Hairer, C. Lubich, and G. Wanner. *Geometric numerical integration: structure-preserving algorithms for ordinary differential equations*, volume 31. Springer Science & Business Media, 2006.
- [28] E. Hairer and G. Wanner. *Solving Ordinary Differential Equations II. Stiff and Differential Algebraic Problems*. Springer Series in Computational Mathematics 14, Springer-Verlag Berlin, 1996.
- [29] P. Jin, L. Lu, Y. Tang, and G. E. Karniadakis. Quantifying the generalization error in deep learning in terms of data distribution and neural network smoothness. *Neural Networks*, 130:85–99, 2020.
- [30] P. Jin, Z. Zhang, A. Zhu, Y. Tang, and G. E. Karniadakis. SympNets: Intrinsic structure-preserving symplectic networks for identifying Hamiltonian systems. *Neural Networks*, 132:166–179, 2020.
- [31] K. Kawaguchi, L. P. Kaelbling, and Y. Bengio. Generalization in deep learning. *arXiv preprint arXiv:1710.05468*, 2017.
- [32] R. T. Keller and Q. Du. Discovery of dynamics using linear multistep methods. *SIAM Journal on Numerical Analysis*, 59(1):429–455, 2021.
- [33] D. P. Kingma and J. Ba. Adam: A method for stochastic optimization. In Y. Bengio and Y. LeCun, editors, *3rd International Conference on Learning Representations, ICLR, San Diego, CA, USA, May 7-9, 2015, Conference Track Proceedings*, 2015.
- [34] J. Z. Kolter and G. Manek. Learning stable deep dynamics models. In *Advances in Neural Information Processing Systems 32: Annual Conference on Neural Information Processing Systems 2019, NeurIPS 2019, December 8-14, 2019, Vancouver, BC, Canada*, pages 11126–11134, 2019.
- [35] Q. Li, L. Chen, C. Tai, and E. Weinan. Maximum principle based algorithms for deep learning. *The Journal of Machine Learning Research*, 18(1):5998–6026, 2017.
- [36] L. Lu, P. Jin, G. Pang, Z. Zhang, and G. E. Karniadakis. Learning nonlinear operators via deepnet based on the universal approximation theorem of operators. *Nature Machine Intelligence*, 3(3):218–229, 2021.
- [37] T. Luo, Z. Ma, Z. J. Xu, and Y. Zhang. Theory of the frequency principle for general deep neural networks. *arXiv preprint arXiv:1906.09235*, 2019.

- [38] M. Raissi, P. Perdikaris, and G. E. Karniadakis. Multistep neural networks for data-driven discovery of nonlinear dynamical systems. *arXiv preprint arXiv:1801.01236*, 2018.
- [39] M. Raissi, P. Perdikaris, and G. E. Karniadakis. Physics-informed neural networks: A deep learning framework for solving forward and inverse problems involving nonlinear partial differential equations. *Journal of Computational Physics*, 378:686–707, 2019.
- [40] S. Reich. Backward error analysis for numerical integrators. *SIAM Journal on Numerical Analysis*, 36(5):1549–1570, 1999.
- [41] R. Rico-Martinez, J. Anderson, and I. Kevrekidis. Continuous-time nonlinear signal processing: a neural network based approach for gray box identification. In *Proceedings of IEEE Workshop on Neural Networks for Signal Processing*, pages 596–605. IEEE, 1994.
- [42] R. Rico-Martinez and I. G. Kevrekidis. Continuous time modeling of nonlinear systems: A neural network-based approach. In *IEEE International Conference on Neural Networks*, pages 1522–1525. IEEE, 1993.
- [43] J. M. Sanz-Serna. Symplectic integrators for hamiltonian problems: an overview. *Acta numerica*, 1:243–286, 1992.
- [44] V. Scheidemann. *Introduction to complex analysis in several variables*. Springer, 2005.
- [45] M. Schmidt and H. Lipson. Distilling free-form natural laws from experimental data. *science*, 324(5923):81–85, 2009.
- [46] Y. Tang. The symplecticity of multi-step methods. *Computers & Mathematics with Applications*, 25(3):83–90, 1993.
- [47] Y. Tong, S. Xiong, X. He, G. Pan, and B. Zhu. Symplectic neural networks in taylor series form for hamiltonian systems. *Journal of Computational Physics*, 437:110325, 2021.
- [48] S. Xiong, Y. Tong, X. He, S. Yang, C. Yang, and B. Zhu. Nonseparable symplectic neural networks. In *9th International Conference on Learning Representations, ICLR 2021, Virtual Event, Austria, May 3-7, 2021*. OpenReview.net, 2021.
- [49] Z. J. Xu, Y. Zhang, and Y. Xiao. Training behavior of deep neural network in frequency domain. In *International Conference on Neural Information Processing*, pages 264–274. Springer, 2019.
- [50] H. Yoshida. Recent progress in the theory and application of symplectic integrators. *Qualitative and Quantitative Behaviour of Planetary Systems*, pages 27–43, 1993.
- [51] H. Yu, X. Tian, Q. Li, et al. Onsagernet: Learning stable and interpretable dynamics using a generalized onsager principle. *arXiv preprint arXiv:2009.02327*, 2020.